A novel sperm-derived seminal fluid protein in *Caenorhabditis* nematodes

Short Title: A novel sperm-derived seminal fluid protein

Katja R. Kasimatis[1,2]*, Christine Rehaluk[1], Locke Rowe[1], and Asher D. Cutter[1]*

[1]Department of Ecology and Evolutionary Biology, University of Toronto, Toronto, Ontario, Canada; [2]Department of Biology, University of Virginia, Charlottesville, VA, USA

*Corresponding authors: kasimatis@virginia.edu (KRK) and asher.cutter@utoronto.ca (ADC)

Acknowledgements: We thank the Phillips lab for sharing plasmids pMS4 and pZCS16 and strain PX814. We thank Zachary Stevenson for transgenic advice, Jack Hu and Mathias Renaud for immunostaining advice, and Stephen Banse, Eric Haag and the Cutter and Claycomb labs for their helpful discussion.

Funding: This research was supported by a Natural Sciences and Engineering Research Council of Canada (NSERC) Banting Postdoctoral Fellowship to KRK and NSERC Discovery Grant Program funding to ADC and LR. The funders had no role in study design, data collection and analysis, decision to publish, or preparation of the manuscript.

Author Contributions: KRK, ADC, and LR devised the project. KRK created strains VX194 and VX300. KRK performed the fecundity assay and experimental evolution. CR performed the immunostaining assays with assistance from KRK. KRK analyzed the data. KRK wrote the manuscript with the support of the other authors.

Data accessibility: The oligonucleotides used in this study are available as Table S1. The immunostaining data are available in File S2 and the complete protocol is available in File S1. The fertility data are available in File S3. The raw amplicon data are available at NCBI SRA under accession number PRJNA1009866. The processed amplicon reads are available in File S4. All scripts are available via the Cutter Lab GitHub repository NSPF (https://github.com/Cutterlab/NSPF). Worm strains JK574 and VX300 are available from the *Caenorhabditis* Genetics Center. Strains PX814 and VX194 are available from the Cutter lab upon request.

The authors declare no conflicts of interest.

ABSTRACT

Nematode sperm contain subcellular vesicles known as membranous organelles (MOs) that fuse with the cell membrane upon sperm activation to release their soluble contents into the extracellular space. The second most abundant proteins in the MOs belong to the conserved Nematode-Specific Peptide family, group F (NSPF) gene family. We hypothesize that these proteins contribute to seminal fluid and are part of post-insemination reproductive tract dynamics. We characterized the anatomical region where the NSPF proteins likely function during fertilization using whole-worm immunostaining of a His-tagged *nspf-1* transgene. We confirmed that NSPF proteins are transferred to females during mating. NSPF proteins localize to the uterus lumen when transferred to mated females and in unmated adult hermaphrodites. These results suggest that the uterine localization of the NSPF proteins is likely a functional property of both male-derived sperm and self-sperm and not incidental to the point of transfer during mating. In males, we found that NSPF presence and abundance was correlated with reproductive maturity. We then used experimental evolution to compete the wildtype allele against a deletion allele in 10 replicate obligate-outcrossing populations. We calculated a mean selective disadvantage of 0.1% for the deletion allele, which indicated that the NSPF genes are beneficial to male fitness. This conclusion was reinforced by qualitative trends from lower powered single-generation fertility assays. Together we demonstrate that nematodes use a novel mechanism for generating seminal fluid proteins and show that the highly abundant NSPF proteins likely have a beneficial impact on fitness.

INTRODUCTION

Post-insemination reproduction studies have largely focused on interactions mediated by seminal fluid. Seminal fluid is a complex mixture of cells, proteins, and other small molecules that are transferred to the female along with sperm (Poiani, 2006; Perry *et al.*, 2013). As a whole, seminal fluid is critical for male fertility – sperm alone is not enough to ensure fertilization – and is implicated in complex behaviors, such as sperm competition, male-female signaling and sexual conflict (Poiani, 2006; McDonough *et al.*, 2016). The study of seminal fluid proteins by evolutionary biologists has largely taken a narrow focus on the study of dozens of *Drosophila* accessory gland proteins (Acps) (Chapman, 2011). The genes underlying many of these Acps are characterized by their elevated evolutionary rate relative to non-reproductive proteins, indicating adaptive evolution through sexually antagonistic coevolution, but also sperm competition (Begun *et al.*, 2000; Swanson & Vacquier, 2002; Clark *et al.*, 2006; Wilburn & Swanson, 2016) or relaxed selection (Dapper & Wade, 2016). However, the null expectation for the evolutionary histories of seminal fluid proteins is not well-developed. Employing new approaches and new taxa may provide a more precise, complete, and generalizable understanding of the complex roles, evolutionary histories, and fitness effects of seminal fluid proteins (Rowe *et al.*, 2018; Hopkins & Perry, 2022).

Caenorhabditis nematodes are a powerful model system for discovering new roles for seminal fluid proteins and expanding our view on the null expectations for their evolutionary histories. First, mating system differs across the genus, with *C. elegans* representing a lineage transition from obligate outcrossing to hermaphroditic self-fertilization (Baldi *et al.*, 2009). In *C. elegans*, males occur in approximately 0.1% of selfed progeny due to X chromosome non-disjunction events, and natural populations show evidence of some outcrossing (Andersen *et al.*, 2012; Félix & Duveau, 2012; Richaud *et al.*, 2018). Both the sperm that derives from males and hermaphrodites are stored in the same region of the gonad of hermaphrodites, allowing for direct competition of sperm types (LaMunyon & Ward, 1998). Using the genetic tools developed in *C. elegans*, researchers can manipulate hermaphrodites to develop as pseudo-females that rely on males to reproduce, which allows direct comparison of the genetics and fitness effects between self-sperm and male-derived sperm to disentangle conflict and cooperation. Additionally, broader contrasts can be made among closely related species with different mating systems and therefore varying opportunities for sexual conflict (Ting *et al.*, 2014; Yin *et al.*, 2018). Second,

53 the small size and rapid generation time of nematodes make them amenable to fitness assays
54 within and across multiple generations. Multi-generation assays allow for detection and
55 quantification of even small fitness effects. Finally, nematodes have unique amoeboid-like
56 crawling sperm which can be visualized through the transparent cuticle, allowing for spectacular
57 live visualization of sperm and seminal fluid dynamics inside of females or hermaphrodites
58 (Smith & Stanfield, 2011; Ting *et al.*, 2014; Hansen *et al.*, 2015; Yin *et al.*, 2018). Very few
59 seminal fluid proteins, however, have been identified and functionally examined in
60 *Caenorhabditis* (Smith & Stanfield, 2011; Yin *et al.*, 2018). Moreover, unlike males in most
61 insect and mammalian systems, nematode males do not have accessory glands specific to
62 seminal fluid production (McGraw *et al.*, 2015), and the anatomical region in which seminal
63 fluid proteins are produced is still unknown. Thus, this system provides an underexploited
64 opportunity for discovering new features of reproductive evolution that can be evaluated and,
65 perhaps, challenge existing paradigms.
66 An intriguing component of nematode sperm cells are subcellular vesicles known as
67 membranous organelles (MOs). In inactive spermatids, MOs are located around the periphery of
68 the cell (Ellis & Stanfield, 2014). Upon ejaculation, spermatids are released from the seminal
69 vesicle and undergo activation as they pass through the vas deferens. During activation, MOs
70 fuse with the cell membrane and create cup-like structures as well as releasing their soluble
71 protein contents into the extracellular space (Ellis & Stanfield, 2014). No accessory gland-like
72 tissues have been identified in *Caenorhabditis* and the source – as well as contents – of seminal
73 fluid are largely unknown (except see Smith & Stanfield, 2011). Consequently, we hypothesize
74 that these MO fusions provide a novel contribution to the seminal fluid proteome.
75 Characterization of the MO proteome identified the Nematode-Specific Peptide family, group F
76 (NSPF) as the second most abundant set of proteins in the MO (Kasimatis *et al.*, 2018).
77 Kasimatis *et al.* (2018) additionally showed that the NSPF genes are conserved in both sequence
78 identity and synteny across the genus. Transcriptomic data support the molecular evolution
79 analyses by capturing NSPF expression in *C. elegans* males along with NSPF ortholog
80 expression in *C. remanei* males (Albritton *et al.*, 2014). High-resolution spatial gene expression
81 mapping localizes NSPF expression to the proximal gonad of adult *C. elegans* males (Ebbing *et*
82 *al.*, 2018). Interestingly, transcriptomic data also identify expression in *C. elegans*

83 hermaphrodites but not *C. briggsae* hermaphrodites, suggesting that this gene family has been
84 incorporated into in at least some self-sperm pathways (Albritton *et al.*, 2014).
85 Here we directly test the hypothesis that MO fusion represents a novel mechanism for
86 contributing proteins to seminal fluid. We use immunostaining of the abundant NSPF proteins as
87 a marker to identify the functional regions that NSPF proteins are associated within males and
88 females/hermaphrodites. We then investigate the impact on fitness of the NSPF gene family
89 using a combination of within generation fertility assays and 20 generations of experimental
90 evolution. Our results indicate that the NSPF proteins are a component of seminal fluid with a
91 marginally-detectable male fitness benefit and imply that even a highly abundant, conserved
92 seminal fluid protein can exert only a subtle function.
93

94 **MATERIALS AND METHODS**

95 **Molecular biology**

96 To create a tagged *nspf-1* gene, guides targeting the sequence in the same intergenic region
97 utilized by the ttTi5650 MosSCI site have previously been described (Dickinson *et al.*, 2015) and
98 inserted into pDD162 (Addgene #47549) to make plasmid pMS4. The repair template plasmid
99 (pKK4) was assembled using the NEBuild HiFi Kit (NEB) from a combination of a restriction
100 digest fragment and a synthetic gBlock Gene Fragment (IDT). The gBlock included the 647 base
101 pairs upstream of *nspf-1* as the promoter region, the *nspf-1* coding sequence with six histidines
102 added before the stop codon, and the *tbb-2* 3' UTR. The plasmid was purified using the GeneJET
103 Plasmid Miniprep Kit (Thermo Scientific) and assembly junctions were verified by Sanger
104 sequencing. A complete list of primers can be found in Table S1.

105 **Strain generation**

106 All strains used in this study are listed in Table S2. The NSPF genes were previously deleted
107 using CRISPR/Cas9 to create strain PX814 (fxDf1 (II: 2,484,339 - 2,487,244)) (Kasimatis *et al.*,
108 2018). To generate an obligate outcrossing deletion strain, JK574 (*fog-2*(q71) V) was crossed
109 with PX814 and then backcrossed 5 times with JK574 to create the obligate outcrossing, deletion
110 strain VX194. The deletion region was verified by Sanger sequencing.
111 Insertion of the His-tagged *nspf-1* transgene was done by CRISPR/Cas9 using standard
112 methods (Dickinson *et al.*, 2015). Briefly, a mixture of 10ng/μL repair template plasmid,
113 50ng/μL plasmid encoding CAS9 and the guide RNA, and 2.5ng/μL of the co-injection plasmid

114 pZCS16 was injected into the gonad of young adult hermaphrodites from PX814. Hygromycin B
115 (BioShop) was added to the injection plates at a final concentration of 250µg/mL three days after
116 injection and hygromycin resistance (HygR) was used as a selectable event. Worms were kept at
117 25ºC for the first five days immediately following injections and then transferred for 20ºC for
118 subsequent generations. Successful insertion was confirmed by PCR (Table S1) and Sanger
119 sequencing. Worms were then backcrossed five times to PX814 to create the final strain VX300
120 (yf*Si*1[*nspf-1*p::*nspf-1*::6xHis::*tbb-2* 3' UTR + loxP, II:8420157]). We tagged the C-terminal of
121 *nspf-1* since these proteins are predicted signaling peptides (Kasimatis *et al.*, 2018) and, thus, the
122 C-terminal is likely included in the mature peptide. The mature peptides for *nspf-1* and *nspf-2*
123 differ by two amino acids and differ by four amino acids between *nsfp-1* and *nspf-3*. These
124 differences are not predicted to change the cleavage site or secondary structure of the peptide.
125 Across the genus, *nspf-1* is more conserved than *nspf-3* (Kasimatis *et al.*, 2018). Thus,
126 expression of *nspf-1* likely is representative of the localization and function of this gene family.

127 **Whole-worm immunohistochemistry**

128 Worms were formaldehyde-fixed and stained following a modified version of the Ruvkun and
129 Finney protocol (WormAtlas). Briefly, worms were cultured at 20ºC on 10cm NGM-agar plates
130 containing 100ng/mL carbenicillin and seeded with formaldehyde killed *E. coli* OP50 (following
131 Beydoun *et al.*, 2021), which was used to reduce non-specific binding of the His-antibody to *E.*
132 *coli* produced histidines. At each developmental stage used, populations of at least 1,000 worms
133 were fixed in a 1% formaldehyde solution and flash frozen in dry ice with ethanol. Incorrect
134 antibody binding was blocked using solution of: 0.3M glycine, 10mM imidazole, 1% BSA, 0.5%
135 skim milk, and 0.25% Triton-X-100 in PBS. Worms were stained for 1 hour at room temperature
136 using a 1/4000 dilution of Recombinant Alex Fluor 488 Anti-6x His Tag antibody (Abcam
137 #ab237336) and co-stained with DAPI. The complete method along with buffer recipes can be
138 found in File S1.

139 To examine the localization of *nspf-1* in males and hermaphrodites across development,
140 VX300 male-rich populations (~40% males) were age synchronized by bleaching (Kenyon,
141 1988) and then formaldehyde-fixed during: L3 (28 hours post-L1), L4 (40 hours post-L1), day 1
142 of adulthood (46 hours post-L1), day 2 of adulthood (70 hours post- L1), and day 8 of adulthood
143 (190 hours post-L1). As a control, JK574 males and pseudo-females were concurrently cultured
144 and fixed at the same developmental stages. In our hands, worms developed more slowly and

less synchronously on plates with dead OP50 than on live OP50. Thus, the exact time in development may be asynchronous between worms, but the developmental stages were accurate. At least 100 stained worms from each strain × sex × developmental stage were scored for the presence and location of fluorescence (File S2). The localization of fluorescence was characterized as occurring in one or more of the following regions: head, distal gonad, proximal gonad (including the spermathecae or seminal vesicle), uterus/vas deferens, vulva/cloaca, or tail. Worms were categorized as "not stained" if no fluorescence was observed.

To determine whether or not males transfer NSPF-1 to females during mating, we crossed JK574 pseudo-females with VX300 males. Both strains were age-synchronized by bleaching followed by isolation of virgin pseudo-females (n = 400) and males (n = 150) during late L4 to 10cm NGM-agar plates containing 100ng/mL carbenicillin and seeded with formaldehyde-killed *E. coli* OP50 (n = 3 replicate plates). Worms were mated overnight and then formaldehyde-fixed and stained. One hundred pseudo-females were scored for the presence and location of fluorescence.

Count data for the presence of fluorescence were analyzed using a χ^2 test based on a contingency table of strain × presence of fluorescence for each sex and developmental stage separately. Specifically, we tested the null hypothesis of no difference between counts of stained individuals and counts of unstained individuals between the control (JK574) and His-tagged (VX300) strains. All analyses were conducted using the R statistical language v4.0.0 (R Core Team, 2020).

Dissected gonad immunohistochemistry

Testes were methanol-fixed and stained following a modified version of the Shakes *et al.* (2009) protocol. Briefly, worms were cultured at 20ºC on 10cm NGM-agar plates and seeded with *E. coli* OP50. Young adult males were decapitated using a 30 gauge needle to release the gonad and then transferred to ColorFrost Plus slides (Fisher Scientific). Gonads were fixed in methanol followed by acetone. Incorrect antibody binding was blocked using solution of: 0.3M glycine, 10mM imidazole, 1% BSA, and 0.25% Triton-X-100 in PBS. Worms were stained for 1 hour at room temperature using a 1/4000 dilution of Recombinant Alex Fluor 488 Anti-6x His Tag antibody (Abcam #ab237336) and co-stained with DAPI. The complete method along with buffer recipes can be found in File S3. Image stacks were processed using ImageJ.

175 **Fertility Assays**

176 We assayed the overall reproductive success of VX194 deletion males late in adulthood. We
177 isolated virgin deletion males on day 1 of adulthood and maintained as virgins until the start of
178 the assay. On day 5 of adulthood, individual males were mated with three wildtype, virgin
179 females (strain JK574) for 24 hours. As a control, wildtype males (strain JK574) were mated to
180 wildtype females following the same timing and male to female ratio. Matings were conducted
181 on small NGM-agar plates (35 mm diameter) seeded with 10µL OP50 *Escherichia coli*. After 24
182 hours, each male was removed and the females were transferred to a new small plate to continue
183 laying eggs. Females were transferred to new plates every 24 hours until progeny production
184 ceased. The total number of progeny was counted as a measure of each male's reproductive
185 success (File S3). Fertility data were analyzed using R (R Core Team, 2020), with the
186 significance of non-competitive reproductive success evaluated using Welch's Two Sample t-test
187 and an analysis of the power of the comparison computed. Previous fecundity data were
188 replotted using the data available in Kasimatis et al. (2018) Additional File 9.

189 **Experimental evolution design and worm culture**

190 To create a base population, reciprocal crosses of virgin females and males from strains JK574
191 and VX194 were performed. The F1 heterozygous progeny were divided into 10 replicate
192 populations of 500 worms with equal numbers of each sex to start the first generation. After
193 generation one, populations were expanded to a census size of N = 1,000 worms per replicate
194 and evolved for 20 generations. To start each generation, age synchronized larval stage 1 (L1)
195 worms were plated onto four 10 cm NGM-agar plates seeded with OP50 *E. coli* at 20ºC with a
196 density of 250 worms per plate (Brenner, 1974; Kenyon, 1988). Worms were left to mate for the
197 first five days of adulthood before eggs were once again collected on day six to synchronize for
198 the next generation. During this mating time, worms within each replicate were pooled and
199 redistributed to fresh NGM-agar plates twice to ensure they never starved. The mating duration
200 provided ample opportunities for females to mate with multiple males. A subset of worms from
201 all replicates was frozen every five generations for future experiments. At generation eight all
202 worms were frozen and the experiment paused for five months due to COVID-19 lockdown
203 restrictions. The thawed population sizes were in excess of the census size and plated at a density
204 of 250 worms per plate, following the regular experimental protocol.

205 **Amplicon sequencing and read calling**

206 We performed amplicon sequencing on pooled samples of 500-800 L1 worms from experimental
207 evolution generations 11 and 20. Two control samples were generated, each with approximately
208 700 worms: 1) F1 heterozygous progeny generated by crossing strains JK574 and VX194, and 2)
209 pooled worms generated by mixing an equal number of JK574 and VX194 worms and sampling
210 from this pool. The wildtype allele was amplified using forward primer (5' to 3')
211 TGCAATGGATTTCTGGTGATAAC and reverse primer (5' to 3')
212 TCTGGCAGTAGGAAAGTGAG, yielding a product of size 230 base pairs. The deletion allele
213 was amplified using forward primer (5' to 3') AGGATAAGAGAGACCCAGAC and reverse
214 primer (5' to 3') TCTGGCAGTAGGAAAGTGAG, yielding a product of size 275 base pairs.
215 PCR products were generated using the OneTaq Quick-Load 2x PCR Master Mix with Standard
216 Buffer (NEB) in accordance with manufacturer instructions with *C. elegans* genomic DNA. PCR
217 products were purified using QIAquick PCR Purification kit (Qiagen) and normalized to
218 20ng/uL. Products were sequenced using GENEWIZ Amplicon-EZ services.

219 Reads for each sample were filtered using bioawk (https://github.com/lh3/bioawk) to
220 exclude reads <50 base pairs in length and with a mean quality score <30. Reads in each sample
221 >230 base pairs in length were then blasted to the deletion reference sequence and retained if the
222 blast score was significant. All remaining reads were then blasted to the unique reference
223 sequence for both the wildtype (bases 1-102) and deletion (bases 1-147) alleles. A read was
224 called as a wildtype or deletion allele based on the best E-value and bit score (File S4). Final
225 counts ranged from 89,721 to 132,685 reads per sample.

226 **Estimating selection**

227 Read data were analyzed using R (R Core Team, 2020) and the *lme4* v.1.13 package (Bates et al.
228 2015). We fit five different linear models. To account for biases during PCR amplification due to
229 different wildtype and deletion product sizes, as suggested by the mean frequency of each allele
230 in the two control samples (*i.e.,* 72.6% wildtype and 27.4% deletion). Models 1-4 only analyzed
231 amplicon sequence data from generations 11 and 20. Model 5 assumed the frequency of each
232 allele to be 50% (*i.e.,* 500 copies of the wildtype allele and 500 copies of the deletion allele for a
233 heterozygous population of N = 500), because all worms were heterozygous at the start of the
234 experiment. Model 6 used the frequency of the deletion allele estimated from the control samples
235 as an alternative generation 1 estimate that includes PCR bias. Model 1 fit read counts over time

236 using a generalized linear mixed model with a binomial logistic distribution and replicate as a
237 random effect: glmer((WT_{count}, DEL_{count}) ~ generation + 1|replicate). We present the results of
238 Models 1 and 6 below as they represent the most conservative estimate of selection. The results
239 of all six models are represented in Table S3 and are qualitatively similar in suggesting a
240 decrease in the frequency of the deletion allele over time.
241
242 **RESULTS**

243 **NSPF proteins localize to the spicules in adult males**

244 We characterized the localization of NSPF proteins during fertilization using whole-worm
245 immunostaining of a His-tagged *nspf-1* transgene re-inserted into the deletion allele background
246 (PX814). We scored the presence of the fluorescent antibody bound to NSPF-1::6xHis in six
247 anatomical regions: head, distal gonad, proximal gonad, vas deferens, cloaca, and tail (Fig. 1A).
248 Throughout male development, we found that NSPF presence and abundance was correlated
249 with male reproductive maturity (Fig. 1B; Fig S1). During larval stage 3 (L3), the gonad is still
250 developing and no staining was present, which supports our previous finding that NSPF
251 production is linked with sperm production (File S2). Sperm production begins during the L4
252 stage and correspondingly some L4 males had staining in both the distal (n = 17 of 126) and
253 proximal gonad (n = 1 of 126; Fig. 2A). Interestingly, 43% of L4 males had staining in the tail
254 region (n = 55 of 126) specifically overlapping with the developing spicules, structures that
255 facilitate mating and sperm transfer in adult males (Emmons, 2005). These patterns are
256 significantly different from control males ($\chi^2 = 175.5$, df = 3, $p < 0.0001$), of which only one
257 individual showed non-specific staining along the cuticle in the proximal gonad region (Fig. 2B).
258 In whole-worm staining of adult males, NSPF proteins localized solely to the spicules
259 (Fig. 2C). Abundance appeared highest on days 1 and 2 of adulthood with 100% of males (n =
260 100 and 150, respectively) showing staining in the tail region (Fig. 1B). Again, these patterns
261 were significantly different from the off-target staining or spicule auto-fluorescence observed in
262 control males during day 1 (n = 13 of 99 stained; $\chi^2 = 149.5$, df = 1, $p < 0.0001$) and day 2 (n =
263 45 of 150 stained; $\chi^2 = 158.5$, df = 1, $p < 0.0001$) of adulthood (Fig. 2D). Older males, however,
264 had a decreased signal of NSPF proteins (n = 59 of 106), though still significantly different from
265 control males ($\chi^2 = 39.4$, df = 1, $p < 0.0001$). This pattern of protein abundance throughout

266 development suggests that NSPF production is tightly correlated with spermatogenesis and peak
267 reproductive output and mating activity during early adulthood.
268 While immunostaining of whole adult worms did not identify NSPF protein within the
269 gonad, dissected testes of adult males confirmed localization of NSPF within spermatids (Fig.
270 S2). The punctate patterning around the nucleus overlaps with the location of MOs, which
271 supports the proteomic characterization of this gene family. Thus, whole worm immunostaining
272 likely lacked the sensitivity to visualize staining within small sperm subcellular structures.

273 **Males transfer NSPF proteins to the female uterus during mating**

274 To test our hypothesis that NSPF proteins form a constituent of seminal fluid, we examined
275 whether males transferred NSPF proteins during mating. Specifically, control pseudo-females
276 (JK574) were mated with His-tagged males (VX300) for 24 hours. Of the pseudo-females
277 without eggs in utero, 38% (n = 8 of 21) had a clear signal of staining around the vulva and in the
278 uterine space (Fig. 3A). This signal was significantly different from that of control females
279 mated to control males ($\chi^2 = 4.9$, df = 1, p = 0.03; Fig. 3B), though given the small sample sizes
280 false positives are possible. Only 12% (n = 15 of 129) of pseudo-females with eggs in utero
281 showed a clear signal of staining, which was not significantly different from pseudo-females
282 mated to control males ($\chi^2 = 0.53$, df = 1, p = 0.47). However, in these females the NSPF
283 proteins appear to be in the uterus lumen, which suggests that eggs may mask the fluorescent
284 signal (Fig. 3C). These results indicate that males transfer NSPF proteins during ejaculation and
285 support the hypothesis that MOs contribute proteins to seminal fluid.

286 **NSPF proteins localize to the uterus of unmated hermaphrodites**

287 To determine if self-sperm NSPF patterns differed from male-derived sperm patterns, we
288 characterized NSPF localization in His-tagged hermaphrodites (VX300) that had been raised in
289 the presence of males throughout development. Again, L3 individuals showed no signal of
290 staining (File S2). L4 hermaphrodites, however, had little to no staining and did not significantly
291 differ from control females (p = 1; Fig. 1C) despite mRNA expression of *nspf-1* during this
292 developmental stage (Harris *et al.*, 2019). The non-overlapping mRNA and protein localization
293 patterns are again likely to be a sensitivity constraint of our whole-animal immunostaining
294 procedure to clearly identify subcellular localization patterns. Adult hermaphrodites all showed
295 the same vulva and uterus localization pattern of staining as we observed in mated, control

296 females (Fig. 1C; Fig. S1). On days 1 and 2 of adulthood, 54% (n = 54 of 100) and 41% (n = 61
297 of 150) of hermaphrodites, respectively, showed staining, which was significantly more than
298 control females (Day 1: $\chi^2 = 49.9$, df = 1, $p < 0.0001$; Day 2: $\chi^2 = 22.6$, df = 1, $p < 0.0001$). On
299 day 8 of adulthood, 67% (n = 90 of 134) of hermaphrodites showed the same significant staining
300 pattern ($\chi^2 = 147.2$, df = 6, $p < 0.0001$; Fig. 1C). Because self-sperm are depleted by day 8 late in
301 adulthood (Hirsh et al. 1976), these data further support the male transfer of NSPF proteins to the
302 uterus. Across all developmental time points, we noted the unexpected absence of signal in the
303 spermathecae, likely due to sensitivity of the whole-worm staining procedure.
304 To distinguish whether the early adulthood signal of NSPF staining was caused by self-
305 fertilization or mating, we examined a male-less population of His-tagged hermaphrodites on day
306 1 of adulthood prior to the start of egg laying. We found that 59% (n = 59 of 100) of
307 hermaphrodites showed the same vulva and uterus pattern of staining (Fig. 3D) despite no
308 opportunity for male transfer of NSPF proteins. This frequency was not significantly different
309 from the number of day 1 hermaphrodites raised in the presence of males ($p = 0.57$). These
310 results suggest that the uterine localization of the NSPF proteins – whether secreted by self-
311 sperm or male sperm – likely reflects their site of activity and not simply a byproduct of the point
312 of transfer during mating.

313 **NSPF genes provide a weak fitness benefit**

314 Having demonstrated that the NSPF proteins are part of seminal fluid, we sought to discover
315 their relationship with reproductive fitness (Fig. S4). Under a model in which expression of *nspf*
316 genes exert a net deleterious effect on females and males, we would expect the evolutionary loss
317 of *nspf* genes from the genomes of species that evolved primarily selfing hermaphroditism (Yin
318 *et al.*, 2018; Cutter *et al.*, 2019), with dynamic patterns of gain and loss for the gene family
319 across species given the high divergence among members of the *Caenorhabditis* genus (Konrad
320 *et al.*, 2018; Stevens *et al.*, 2020). Alternatively, under a model in which NSPF activity is
321 selectively-neutral, we would expect to see a lack of constraint in the sequence evolution and
322 copy number dynamics of this gene family (Kimura, 1968). However, the signatures of
323 conservation of amino acid sequence and synteny indicating purifying selection (Kasimatis *et al.*,
324 2018) are consistent with neither a deleterious nor a neutral model. Instead, they suggest a net
325 fitness benefit mediated by one or both sexes. If the NSPF proteins were neutral or beneficial to
326 male reproductive function but costly to female reproductive function, then we would expect: 1)

327 self-sperm derived NSPF expression to be lost or significantly reduced (Yin *et al.*, 2018; Cutter
328 *et al.*, 2019), and/or 2) dynamic molecular evolution of the gene family across the phylogeny due
329 to heterogeneity in the net balance of male benefit to female cost. Given the NSPF phylogenetic
330 conservation (Kasimatis *et al.*, 2018) as well as conservation of self-sperm derived NSPF at the
331 transcriptional level (Ebbing *et al.*, 2018) and protein level (Fig. 3D), we hypothesize that the
332 NSPF proteins benefit reproductive fitness and that this benefit is directed toward both female
333 and male reproduction (Fig. S4).

334 Previous experiments on male fertility as young adults showed no significant difference
335 in total fecundity between wildtype males and males with all three copies of the NSPF genes
336 deleted (*i.e.,* deletion allele) (Fig. S3A; Kasimatis *et al.*, 2018). Using old males (day 5 of
337 adulthood), we repeated these non-competitive, total fecundity assays to determine whether
338 NSPF proteins improved male sperm fertilization ability in a late phase of the life cycle when
339 male fertility is declining overall. Although the mean fecundity of old males with the deletion
340 allele trended lower than wildtype males (x_{del} = 459; x_{wt} = 481.9), the effect was not significant
341 (p = 0.85; Fig. S3A). This nominal decrease in fecundity of males with the deletion allele was
342 similar to what was previously seen with young adult males under a competitive male setting,
343 suggesting that NSPF function is potentially both age-independent and sperm competition-
344 independent (Kasimatis et al. 2018; Fig. S3B). Given the experiment size and high reproductive
345 variance, however, a difference between genotypes of 71% would be required to achieve 80%
346 power to detect a significant difference. Nonetheless, the within-generation trends suggest that
347 these proteins are either beneficial or neutral with regards to both male and female fitness,
348 despite the high abundance of the proteins. The null results of these late-life assays coupled with
349 the previous early-life assays (Kasimatis *et al.*, 2018) provide no evidence that these proteins are
350 costly to females as the fecundity of females mated with deletion males did not increase in three
351 independent experiments.

352 We turned to experimental evolution to overcome the power limitations of within-
353 generation experimental design and test whether the NSPF genes are male-beneficial or male-
354 neutral. Specifically, we competed the wildtype allele against the deletion allele in an obligate
355 outcrossing *C. elegans* population by evolving ten replicate populations of 1,000 individuals
356 from a base population that was heterozygous at the NSPF locus in an otherwise homogeneous
357 genetic background. Between generations 11 and 20, we documented a significant overall

358 decrease in the frequency of the deletion allele across replicates (GLM Model 1: z-value = -2.9, p
359 = 0.003) with the deletion allele clearly decreasing in frequency by at least 4% in four of the ten
360 replicates and remaining approximately the same in two replicates (≤ 2% change). Between
361 replicate effects accounted for 27% of the variance observed. When including the sequencing
362 control samples as a technical estimate of the allele frequencies at generation 1, no significant
363 allele frequency change is observed over time, suggesting a more neutral fitness effect of the
364 NSPF protein (Fig. 4; Table S3). These results support the within-generation fecundity trends to
365 indicate that any effect of males transferring NSPF protein to females does not impose a large
366 fitness cost to females. Instead, under these conditions, we estimate the wildtype allele to confer
367 approximately a 0.1% fitness advantage over the deletion allele (Table S3). Together, these
368 proteins appear to provide an overall weak net fitness effect that is consistent with being
369 beneficial or neutral to females and males (Fig. S4).
370

371 **DISCUSSION**

372 Seminal fluid is a complex bioactive mixture whose components are implicated in a variety of
373 reproductive, behavioral and physiological functions and thus likely evolves in response to
374 multiple selective pressures. We took an integrative approach to investigate the highly abundant
375 MO-associated NSPF proteins. We confirmed that the NSPF genes are indeed a component of
376 seminal fluid that is transferred to females, which demonstrates that MO fusion provides a novel
377 source of seminal fluid proteins. Additionally, the localization of NSPF proteins (*i.e.,* the
378 functional output) differs from that of mRNA transcripts, which is consistent with ejaculate
379 proteins and not sperm-specific proteins. Finally, using within- and across-generation
380 experiments, we quantified the small, but significant contribution made to reproductive fitness by
381 the presence of NSPF proteins, most consistent with a positive fitness effect in males and either a
382 positive or neutral fitness effect in females (Fig. S4). Together, this work demonstrates the power
383 of *Caenorhabditis* to expand our perspective of seminal fluid protein function and to disentangle
384 beneficial versus antagonistic effects of seminal fluid proteins.

385 The localization of NSPF protein to the spicule (Fig. 2) and uterus (Fig. 3) was
386 unexpected given that the NSPFs were previously characterized as being associated with sperm
387 MOs (Kasimatis *et al.*, 2018) and that mRNA expression data indicated that all three *nspf* genes
388 are expressed in the gonad only (Ebbing *et al.*, 2018). Staining of dissected testes provided the

389 necessary sensitivity to confirm that NSPF proteins localize to spermatid MOs. Our whole-worm
390 staining approach did, however, identify additional regions of localization that may result from
391 the anatomical difference in the location of inactivated versus activated sperm. The activation
392 process occurs as sperm pass from a male to a female/hermaphrodite while the spicules are
393 everted in the vulva, thus creating a direct link between MO fusion and the spicules. This overlap
394 in timing, however, does not explain the spicule signal seen in L4 larval males, which warrants
395 further work. In hermaphrodites, the parsimonious hypothesis is that NSPF proteins passively
396 diffuse from the spermathecae, where activated sperm reside, to the uterus. The location of NSPF
397 proteins within the uterus is similar to other proteins that males transfer, which originate in
398 newly identified extracellular vesicles (Nikonorova *et al.*, 2022). While the NSPFs do not appear
399 in these vesicles, it is possible that this alternative vesicle type also contributes to seminal fluid
400 proteins, supporting our finding that nematodes employ a distinct mechanism for secreting
401 seminal fluid proteins than either mammals or *Drosophila* (McGraw *et al.*, 2015).
402 We capitalized on the ability to manipulate mating system to show that NSPF production
403 is not only retained during the lineage transition to self-fertilization, but that the proteins localize
404 to the same uterus region in unmated hermaphrodites as in mated females (Fig. 3). This pattern
405 reinforces the pattern of conserved molecular evolution of the *nspf* gene sequences (Kasimatis *et*
406 *al.*, 2018) and implies that the reproductive function of the sperm-dependent NSPF proteins
407 within the uterus is mating-independent. Importantly, the conserved expression during
408 spermatogenesis in L4 hermaphrodites relative to males of the ancestral gonochoristic species
409 supports the notion that these proteins are not involved in ongoing sexual conflict, as there would
410 be strong selection favoring their loss as seen in many other male reproductive traits (Thomas *et*
411 *al.*, 2012; Fierst *et al.*, 2015; Yin *et al.*, 2018). Instead, expression of *nspf* genes appear beneficial
412 to reproductive fitness, if weakly, as supported by fitness assays. If their net advantage resulted
413 from a detriment to females that was offset by a male fitness benefit, then we would expect
414 females mated with deletion males to trend toward higher reproductive success than females
415 mated with wildtype males. However, our experiments support the opposite of such a scenario,
416 suggesting NSPF promotes sexually-concordant reproductive fitness.
417 A common challenge in evolutionary biology is to detect the fitness effects of variants at
418 a single gene (Barrett & Hoekstra, 2011). Our experimental evolution design to compete the
419 wildtype and deletion alleles in a highly-replicated fashion allowed for the potential to

420 compound small effect sizes over tens of generations. The nematode model system allows for
421 this approach to be done at a larger scale and over a longer time periods than similar studies
422 (Wong & Rundle, 2013), which, when coupled with genomics, provides greater power to detect
423 small or fluctuating selection coefficients that are most likely to underlie allelic effects in
424 standing genetic variation. The overall trend across replicates was a slight decrease in the
425 frequency of the deletion allele (Fig. 4). The estimated selection coefficient, despite being small,
426 would be powerful enough to prevent *nspf* gene loss over time in nature. Such a small fitness
427 effect is surprising given the molecular evolutionary history of these genes, but supports the
428 "mild phenotype" observed in many classic genetics knockout/knockdown studies (Sugimoto,
429 2004; Bell, 2010). The frequency of the deletion allele did not decrease consistently in every
430 replicate at each sampling time point, however, which likely reflected a combination of variance
431 and stochasticity during mating along with sampling error and the relatively small selection
432 coefficient. Additionally, the ability of females to mate with multiple males created the
433 opportunity for wildtype males to compensate for any benefits a female lost by mating with a
434 deletion male. Such compensation would dampen the effect of selection against the deletion
435 allele and potentially contribute to the fluctuating frequency of the deletion allele. Overall, this
436 approach of allelic competition in experimental evolution (Gray & Cutter, 2014; Teotonio *et al.*,
437 2017) may represent a promising avenue for future seminal fluid protein studies, and for genetic
438 variants of other phenotypes, where small fitness effect sizes have proved challenging to
439 characterize.

440 Our data motivate multiple hypotheses for future testing to narrow down the specific
441 beneficial function of the NSPF proteins. First, the NSPF proteins could interact with a male-
442 female signaling network that promotes egg laying. While the interacting partner for NSPF
443 proteins remains unknown, it is possible that NSPFs bind to muscle proteins that form the uterus
444 walls and are involved in egg laying behavior. Under this hypothesis, localization to the spicules
445 is puzzling. However, previous work has shown the females pressurize the gonad to push some
446 of the ejaculate mass and spicules out of the vulva (Barker, 1994; Kleemann & Basolo, 2007).
447 This process could create a residue on the spicule cuticle as a byproduct, though we cannot rule
448 out a functional relationship between the NSPF proteins and spicule cuticle.

449 Alternatively, the NSPF proteins could impact the uterine environment. Specifically,
450 seminal fluid of some species contains anti-microbial factors (Samakovlis *et al.*, 1991; Gao &

Zhu, 2016). Given the density of protein right above the vulva, one hypothesis is that the NSPF proteins play an anti-microbial role to protect the uterus from bacterial infection. Previous work has shown that the uterus can be exposed to pathogenic infection from the external environment during mating and egg laying (Muir & Tan, 2008). The male spicules are presumably also exposed during eversion, and thus any anti-microbial activity of the NSPF residue on the spicules might serve to prevent bacterial infection in males when the spicules retract. Biochemically, the alpha-helix structure of NSPF proteins lends plausibility to this hypothesis, as such secondary structures can confer generic bacterial lysing properties (Huan *et al.*, 2020). Future work testing the fitness effects of the NSPF deletion allele in worms raised in environments with more pathogenic bacteria is warranted.

Our work demonstrates the complex but subtle dynamics of seminal fluid proteins uncovered when using integrative approaches. We also showed how *Caenorhabditis* nematodes are an excellent system for expanding our knowledge of post-insemination interactions not only for their technical benefits, but also for their novel sperm components and potential for distinguishing sexual conflict from sexual cooperation by making mating system contrasts between male-derived sperm and self-sperm interactions. Connecting the layers of the genotype-phenotype-fitness map for seminal fluid proteins will help us uncover the genetics of fertility and the evolution of reproductive success.

470 **References**

471 Albritton, S.E., Kranz, A.-L., Rao, P., Kramer, M., Dieterich, C. & Ercan, S. 2014. Sex-biased
472 gene expression and evolution of the x chromosome in nematodes. *Genetics* **197**: 865–883.
473 Andersen, E.C., Gerke, J.P., Shapiro, J.A., Crissman, J.R., Ghosh, R., Bloom, J.S., *et al.* 2012.
474 Chromosome-scale selective sweeps shape *Caenorhabditis elegans* genomic diversity. *Nat*
475 *Rev Genet* **44**: 285–290.
476 Baldi, C., Cho, S. & Ellis, R.E. 2009. Mutations in two independent pathways are sufficient to
477 create hermaphroditic nematodes. *Science* **326**: 1002–1005.
478 Barker, D.M. 1994. Copulatory plugs and paternity assurance in the nematode *Caenorhabditis*
479 *elegans*. *Animal Behaviour* **48**: 147–156.
480 Barrett, R.D.H. & Hoekstra, H.E. 2011. Molecular spandrels: tests of adaptation at the genetic
481 level. *Nat Rev Genet* **12**: 767–780.
482 Begun, D.J., Whitley, P., Todd, B.L., Waldrip-Dail, H.M. & Clark, A.G. 2000. Molecular
483 population genetics of male accessory gland proteins in *Drosophila*. *Genetics* **156**: 1879–
484 1888.
485 Bell, G. 2010. Experimental genomics of fitness in yeast. *Proc. R. Soc. B: Biol. Sci.* **277**: 1459–
486 1467.
487 Beydoun, S., Choi, H.S., Dela-Cruz, G., Kruempel, J., Huang, S., Bazopoulou, D., *et al.* 2021.
488 An alternative food source for metabolism and longevity studies in *Caenorhabditis elegans*.
489 *Commun Biol* **4**: 258–9.
490 Brenner, S. 1974. The genetics of *Caenorhabditis elegans*. *Genetics* **77**: 71–94.
491 Chapman, T. 2011. Seminal fluid-mediated fitness traits in *Drosophila*. *Heredity* **87**: 511–521.
492 Clark, N.L., Aagaard, J.E. & Swanson, W.J. 2006. Evolution of reproductive proteins from
493 animals and plants. *Reproduction* **131**: 11–22.
494 Cutter, A.D., Morran, L.T. & Phillips, P.C. 2019. Males, Outcrossing, and Sexual Selection in
495 Caenorhabditis Nematodes. *Genetics* **213**: 27–57.
496 Dapper, A.L. & Wade, M.J. 2016. The evolution of sperm competition genes: The effect of
497 mating system on levels of genetic variation within and between species. *Evolution* **70**: 502–
498 511.
499 Dickinson, D.J., Pani, A.M., Heppert, J.K., Higgins, C.D. & 2015. 2015. Streamlined genome
500 engineering with a self-excising drug selection cassette. *Genetics* **200**: 1035–1049.

501 Ebbing, A., Vértesy, Á., Betist, M.C., Spanjaard, B., Junker, J.P., Berezikov, E., *et al.* 2018.
502 Spatial transcriptomics of *C. elegans* males and hermaphrodites identifies sex-specific
503 differences in gene expression patterns. *Developmental Cell* **47**: 801–813.
504 Ellis, R.E. & Stanfield, G.M. 2014. The regulation of spermatogenesis and sperm function in
505 nematodes. *Sem Cell Dev Biol* **29**: 17–30.
506 Emmons, S.W. 2005. Male development. *WormBook* 1–22.
507 Félix, M.-A. & Duveau, F. 2012. Population dynamics and habitat sharing of natural populations
508 of *Caenorhabditis elegans* and *C. briggsae*. *BMC Biol.* **10**: 59.
509 Fierst, J.L., Willis, J.H., Thomas, C.G., Wang, W., Reynolds, R.M., Ahearne, T.E., *et al.* 2015.
510 Reproductive mode and the evolution of genome size and structure in *Caenorhabditis*
511 nematodes. *PLoS Genetics* **11**: e1005323.
512 Gao, B. & Zhu, S. 2016. The drosomycin multigene family: three-disulfide variants from
513 Drosophila takahashii possess antibacterial activity. *Nat Rev Genet* **6**: 32175.
514 Gray, J.C. & Cutter, A.D. 2014. Mainstreaming *Caenorhabditis elegans* in experimental
515 evolution. *Proc Royal Soc B Biological Sci* **281**: 20133055.
516 Hansen, J.M., Chavez, D.R. & Stanfield, G.M. 2015. COMP-1 promotes competitive advantage
517 of nematode sperm. *eLife* 1–26.
518 Harris, T.W., Arnaboldi, V., Cain, S., Chan, J., Chen, W.J., Cho, J., *et al.* 2019. WormBase: a
519 modern model organism information resource. *Nucleic Acids Research* **29**: 82.
520 Hopkins, B.R. & Perry, J.C. 2022. The evolution of sex peptide: sexual conflict, cooperation, and
521 coevolution. *Biological Reviews* **97**: 1426–1448.
522 Huan, Y., Kong, Q., Mou, H. & Yi, H. 2020. Antimicrobial peptides: classification, design,
523 application and research progress in multiple fields. *Front Microbiol* **11**: 582779.
524 Kasimatis, K.R., Moerdyk-Schauwecker, M.J., Timmermeyer, N. & Phillips, P.C. 2018.
525 Proteomic and evolutionary analyses of sperm activation identify uncharacterized genes in
526 *Caenorhabditis* nematodes. *BMC Genomics* **19**: 593.
527 Kenyon, C. 1988. The Nematode *Caenorhabditis elegans*. *Science* **240**: 1448–1453.
528 Kimura, M. 1968. Evolutionary rate at the molecular level. *Nature* **217**: 624–626.
529 Kleemann, G.A. & Basolo, A.L. 2007. Facultative decrease in mating resistance in
530 hermaphroditic *Caenorhabditis elegans* with self-sperm depletion. *Anim Behav* **74**: 1339–
531 1347.

532 Konrad, A., Flibotte, S., Taylor, J., Waterston, R.H., Moerman, D.G., Bergthorsson, U., *et al.*
533 2018. Mutational and transcriptional landscape of spontaneous gene duplications and
534 deletions in *Caenorhabditis elegans*. *Proc. Natl. Acad. Sci.* **115**: 7386–7391.
535 LaMunyon, C.W. & Ward, S. 1998. Larger sperm outcompete smaller sperm in the nematode
536 *Caenorhabditis elegans*. *Proc R Soc Lond B* **265**: 1997–2002.
537 McDonough, C.E., Whittington, E., Pitnick, S. & Dorus, S. 2016. Proteomics of reproductive
538 systems: Towards a molecular understanding of postmating, prezygotic reproductive
539 barriers. *J. Proteomics* **135**: 26–37.
540 McGraw, L.A., Suarez, S.S. & Wolfner, M.F. 2015. On a matter of seminal importance.
541 *Bioessays* **37**: 142–147.
542 Muir, R.E. & Tan, M.-W. 2008. Virulence of *Leucobacter chromiireducens* subsp. *solipictus* to
543 *Caenorhabditis elegans*: characterization of a novel host-pathogen interaction. *Appl Environ*
544 *Microbiol* **74**: 4185–4198.
545 Nikonorova, I.A., Wang, J., Cope, A.L., Tilton, P.E., Power, K.M., Walsh, J.D., *et al.* 2022.
546 Isolation, profiling, and tracking of extracellular vesicle cargo in *Caenorhabditis elegans*.
547 *Curr. Biol.* **32**: 1–13.
548 Perry, J.C., Sirot, L. & Wigby, S. 2013. The seminal symphony: how to compose an ejaculate.
549 *Trends Ecol Evol* **28**: 414–422.
550 Poiani, A. 2006. Complexity of seminal fluid: a review. *Behav Ecol Sociobiol* **60**: 289–310.
551 Richaud, A., Zhang, G., Lee, D., Lee, J. & Félix, M.-A. 2018. The local coexistence pattern of
552 selfing genotypes in *Caenorhabditis elegans* natural metapopulations. *Genetics* **208**: 807–
553 821.
554 Rowe, L., Chenoweth, S.F. & Agrawal, A.F. 2018. The genomics of sexual conflict. *Am Nat* **192**:
555 274–286.
556 Samakovlis, C., Kylsten, P., Kimbrell, D.A., Engström, A. & Hultmark, D. 1991. The andropin
557 gene and its product, a male-specific antibacterial peptide in *Drosophila melanogaster*. *The*
558 *EMBO Journal* **10**: 163–169.
559 Shakes, D.C., Wu, J., Sadler, P.L., LaPrade, K., Moore, L.L., Noritake, A., *et al.* 2009.
560 Spermatogenesis-specific features of the meiotic program in *Caenorhabditis elegans*. *Plos*
561 *Genet* **5**: e1000611.

562 Smith, J.R. & Stanfield, G.M. 2011. TRY-5 Is a sperm-activating protease in *Caenorhabditis*
563 *elegans* seminal fluid. *PLoS Genetics* **7**: e1002375.
564 Stevens, L., Rooke, S., Falzon, L.C., Machuka, E.M., Momanyi, K., Murungi, M.K., *et al.* 2020.
565 The genome of *Caenorhabditis bovis*. *Curr. Biol.* **30**: 1023-1031.e4.
566 Sugimoto, A. 2004. High-throughput RNAi in *Caenorhabditis elegans*: genome-wide screens
567 and functional genomics. *Differentiation* **72**: 81–91.
568 Swanson, W.J. & Vacquier, V.D. 2002. Reproductive protein evolution. *Annu. Rev. Ecol. Syst.*
569 **33**: 161–179.
570 Team, R.C. 2020. *R: A language and environment for statistical computing*. Foundation for
571 Statistical Computing.
572 Teotonio, H., Estes, S., Phillips, P.C. & Baer, C.F. 2017. Experimental evolution with
573 *Caenorhabditis* nematodes. *Genetics* **206**: 691–716.
574 Thomas, C.G., Li, R., Smith, H.E., Woodruff, G.C., Oliver, B. & Haag, E.S. 2012. Simplification
575 and desexualization of gene expression in self-fertile nematodes. *Current Biology* **22**: 2167–
576 2172.
577 Ting, J.J., Woodruff, G.C., Leung, G., Shin, N.-R., Cutter, A.D. & Haag, E.S. 2014. Intense
578 sperm-mediated sexual conflict promotes reproductive isolation in *Caenorhabditis*
579 nematodes. *PLoS Biol* **12**: e1001915-14.
580 Wilburn, D.B. & Swanson, W.J. 2016. From molecules to mating: Rapid evolution and
581 biochemical studies of reproductive proteins. *J. Proteomics* **135**: 12–25.
582 Wong, A. & Rundle, H. 2013. Selection on the *Drosophila* seminal fluid protein Acp62F. *Ecol*
583 *Evol* **3**: 1942–1950.
584 Yin, D., Schwarz, E.M., Thomas, C.G., Felde, R.L., Korf, I.F., Cutter, A.D., *et al.* 2018. Rapid
585 genome shrinkage in a self-fertile nematode reveals sperm competition proteins. *Science*
586 **359**: 55–61.
587

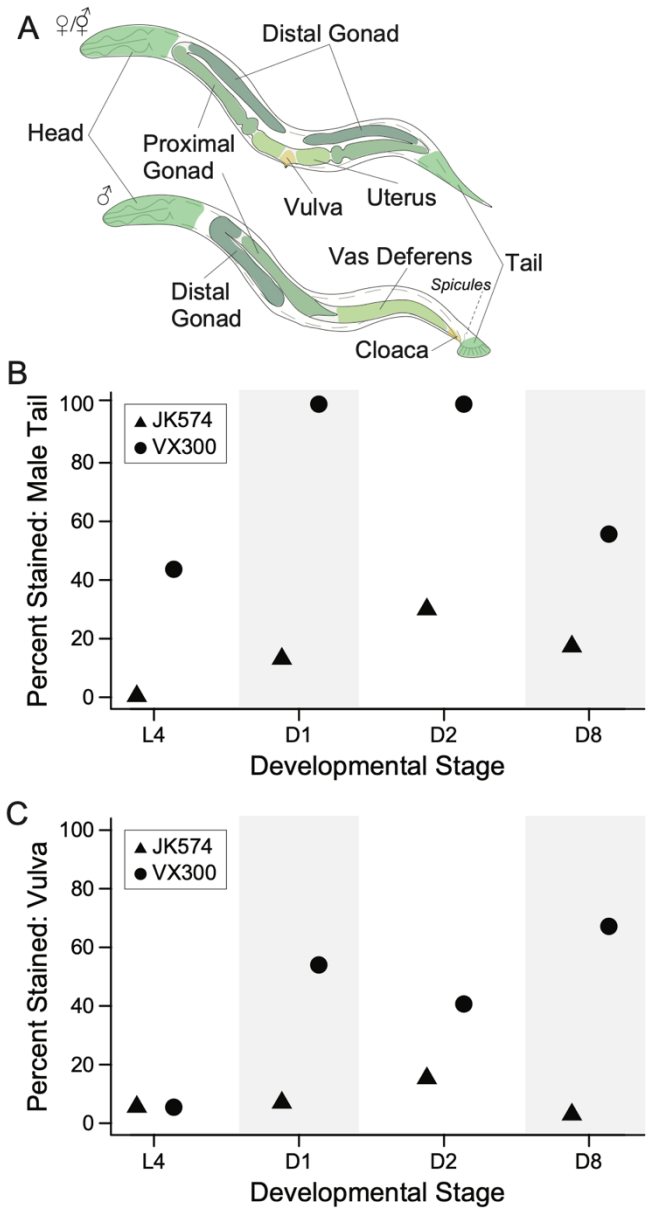

Figure 1. Quantification of antibody staining of 6x His-tagged NSPF-1. A) Diagram of the anatomical regions scored for presence of fluorescence in hermaphrodites/females and males. **B)** The percent of control males (JK574, triangle) and His-tagged males (VX300, circle) with fluorescence in the tail region during larval stage 4 (L4), day 1 of adulthood (D1), day 2 of adulthood (D2), and day 8 of adulthood (D8). **C)** The percent of control females (JK574, triangle) and His-tagged hermaphrodites (VX300, circle) with fluorescence in the vulva region during larval stage 4 (L4), day 1 of adulthood (D1), day 2 of adulthood (D2), and day 8 of adulthood (D8). Immunostaining counts across all anatomical regions is shown in Fig. S1.

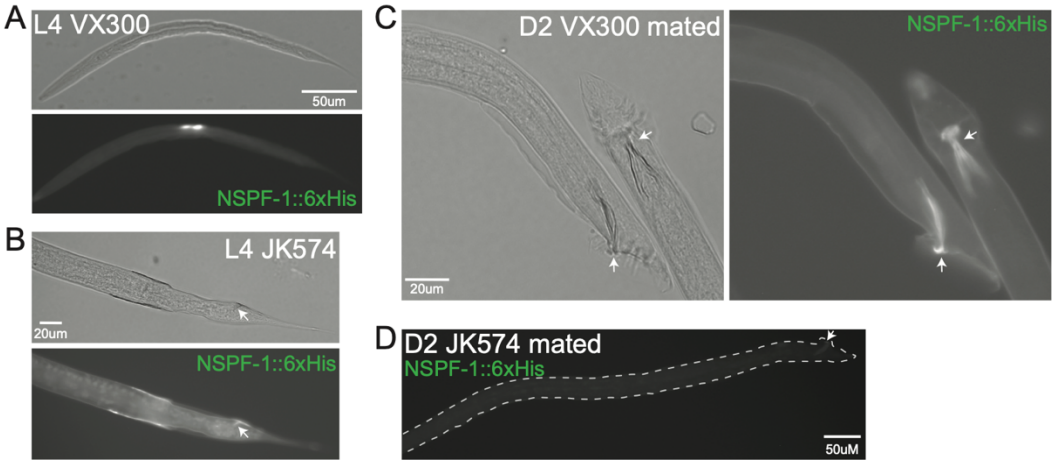

Figure 2. NSPF-1 localizes the spicules of adult males. A) Protein localized to the gonad of L4 His-tagged males. **B)** L4 control males showed off-target staining, predominantly in the cuticle including the cuticle adjacent to the spicules, but not in the spicules. **C)** In adult His-tagged males, protein localized to the spicule structure in the male tail region. **D)** In adult control males, low levels of autofluorescence are detected in the spicules. However, the signal is markedly different than seen in His-tagged males. In all images, the arrow points to the spicule.

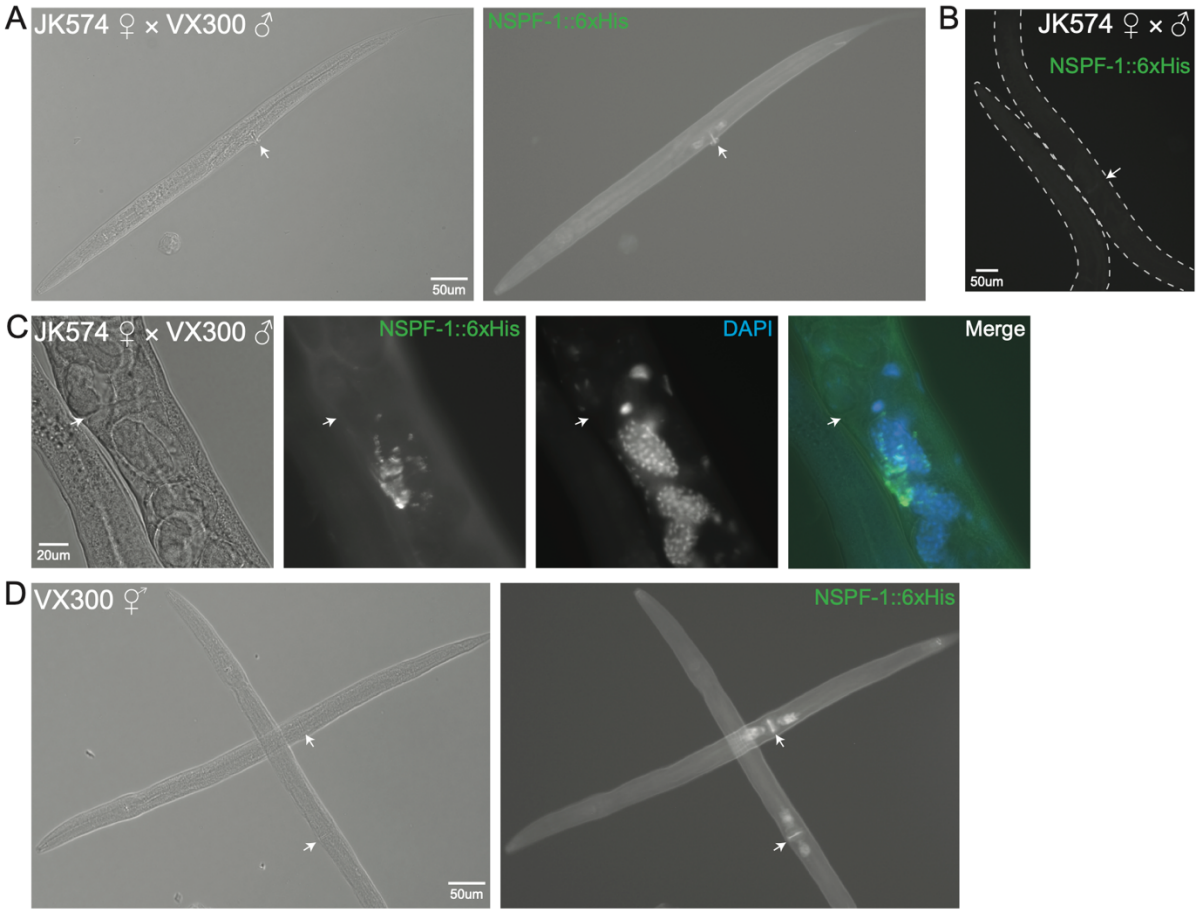

Figure 3. NSPF-1 localizes to the vulva and uterus of mated females and adult hermaphrodites. A) Control pseudo-females mated to His-tagged males showed evidence of protein localization in the vulva and uterus, especially when eggs were not yet present in the uterus. **B)** Control pseudo-females mated to control males showed no evidence of staining. **C)** Control pseudo-females mated with eggs present in the uterus after mating with His-tagged males also had protein present in the uterus, though the signal was not always clear. However, when present the proteins seemed to localize to the lumen and potentially along the surface of vulva muscle cells, as shown in the merged image. **C)** His-tagged adult hermaphrodites who had never been mated by a male showed the same protein localization in the uterus. In all images, the arrow points to the vulva.

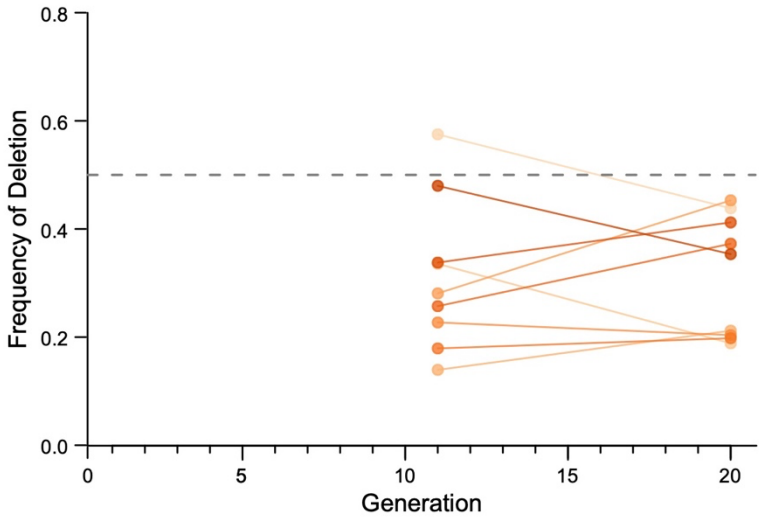

Figure 4. Changes in the frequency of the deletion allele over time estimated using amplicon sequencing data. All ten replicates started with 50% deletion allele (dashed line). The orange points represent the frequency of the deletion allele in each replicate population empirically estimated from amplicon sequence data collected at generations 11 and 20. Statistical testing of the empirical observations used a general linear model (Table S3). There was a significant decrease in the frequency of the deletion allele between generations 11 and 20 (GLM Model 1: $s = 0.001$, z-value = -2.98, $p < 0.01$).

625 **Supplemental Files**

626 **Fig S1. Immunostaining quantification development. A)** Count data showing the percent of
627 control males (JK574, triangle) and His-tagged males (VX300, circle) with fluorescence in each
628 anatomical region during larval stage 4 (L4, orange), day 1 of adulthood (D1, green), day 2 of
629 adulthood (D2, blue), and day 8 of adulthood (D8, pink). **C)** Count data showing the percent of
630 control females (JK574, triangle) and His-tagged hermaphrodites (VX300, circle) with
631 fluorescence in each anatomical region during larval stage 4 (L4, orange), day 1 of adulthood
632 (D1, green), day 2 of adulthood (D2, blue), and day 8 of adulthood (D8, pink).

633

634 **Fig S2. NSPF-1 localizes the MOs of spermatids in adult males. A)** Protein (green) localized
635 in a punctate pattern around the nucleus (blue) of spermatids in the dissected testes of adult His-
636 tagged males. **B)** Protein localization within a single spermatid (outlined) of an adult His-tagged
637 male. **C)** Protein localization within multiple spermatids (arrows) of an adult His-tagged male.

638

639 **Fig S3. Single male fecundity assays. A)** The total fecundity of wildtype males with the NSPF
640 genes (gray) and deletion males with the NSPF genes removed (orange) at day 1 of adulthood
641 and day 5 of adulthood. There was no significant difference in reproductive success between
642 male types. Day 1 data were replotted from Kasimatis et al. (2018). **B)** The proportion of
643 progeny coming from wildtype males (gray) or deletion males (orange) versus a wildtype
644 competitor male. There was no significant difference in sperm competitive ability between male
645 types (Kasimatis et al. 2018). Competitive fecundity success data were replotted from Kasimatis
646 et al. (2018).

647

648 **Fig S4. Summary of evidence for the fitness effect of NSPF in each sex.** We present the
649 expected pattern of sequence evolution, gene expression, immunostaining, sperm biology, and
650 allele frequency for each combination of NSPF effects on males and females. The lines of
651 evidence supporting or contrary to that combination of effects is then given. The evidence most
652 strongly supports a fitness model of male beneficial and female beneficial or neutral.

653

654 **Table S1. Primers used in this study.**

655 **Table S2. Strains used in this study.**

656 **Table S3. Model comparison for amplicon sequencing data.**

657

658 **File S1. Complete immunostaining protocols and buffer recipes.**

659 **File S2. Immunostaining data.**

660 **File S3. Late life fecundity data.**

661 **File S4. Processed amplicon reads.**